Nuclear Transport by Laser-Induced Pressure Transients

Tai-Yuan David Lin,[1] Daniel J. McAuliffe,[1] Norm Michaud,[1] Hong Zhang,[1] Shun Lee,[1] Apostolos G. Doukas,[1] and Thomas J. Flotte[1,2]

Received February 11, 2003; accepted February 24, 2003

Purpose. Control of the transport of molecules into the nucleus represents a key regulatory mechanism for differentiation, transformation, and signal transduction. Permeabilization of the nuclear envelope by physical methods can have applications in gene therapy. Laser-induced pressure transients can produce temporary aqueous pores analogous to those produced by electroporation and that the cells can survive this procedure. In this study, we examine the role of the pressure transients in creating similar pores in the nuclear envelope.

Methods. The target human peripheral blood mononuclear cells in a 62 μM 72 kDa fluoresceinated dextran solution were exposed to the pressure transients generated by laser ablation. An *in vitro* fluorescence confocal microscope was used to visualize and quantify the fluoresceinated dextran in the cytoplasmic and nuclear compartments.

Results. In contrast to electroporation, the pressure transients could deliver 72 kDa fluoresceinated dextrans, which are normally excluded by the nucleus, across the nuclear envelope into the nucleus. In addition to creating pores in the plasma membrane, temporary pores were also created in the nuclear envelope following exposure to pressure transients.

Conclusion. The production of temporary nuclear pores could provide a unique resource for drug-delivery and gene therapy.

KEY WORDS: drug delivery; nuclear envelope; ablation; shock waves; electroporation.

INTRODUCTION

The nuclear envelope separates the nucleus from the cytoplasm. As part of the functional network of the eukaryotic cell, the nuclear envelope facilitates the exchange of regulatory and instructive molecules between the genetic material in the nucleus and the cytoplasm (1). Control of the transport of proteins into the nucleus represents a key regulatory mechanism for differentiation, transformation, and signal transduction.

Transport of small molecules (<17 kDa) occurs by passive diffusion through the nuclear pore complexes. Larger molecules (>41 kDa) require a nuclear localizing sequence and an active transport process to be transported into the nucleus (2). For exogenous compounds such as dextrans the nuclear envelope behaves like a molecular sieve with a functional pore radius of 5 to 6 nm (1–5). Dextrans are spherical, hydrophilic, and inert molecules that have little tendency to be bound or degraded within cells (2,3). They are particularly suited to measure translational mobility and transport between the cytoplasm and nucleus (2,3). On injection into cytoplasm of the cell, it has been shown that the dextrans <17.5 kDa were distributed to the same concentration in the nucleus and the cytoplasm, whereas those >41 kDa were limited to the cytoplasm (3,5,6).

Laser-induced pressure transients have been shown to transiently permeabilize the plasma membrane without causing cytotoxicity (7). In this study, we demonstrated that pressure transients can also permeabilize the nuclear envelope. Fluorescence confocal microscopy with its thin optical sectioning capability was used to visualize and quantify the fluoresceinated 72 kDa dextran in the cytoplasmic and nuclear compartments. The 72 kDa dextran, with an average molecular mass larger than the nuclear exclusion limit for passive diffusion, was present in the nucleus, following the laser-induced pressure transients. These images were compared with those produced by electroporation, a gold standard for DNA transfection.

MATERIALS AND METHODS

Cell Preparation

Human peripheral blood mononuclear cells (PBMC) were used as target cells. Blood was drawn in a heparinized syringe from healthy human volunteers. The blood was mixed with Dulbecco's phosphate buffered saline (PBS) without Ca^{2+} and Mg^{2+}. The blood suspension was carefully layered onto a ficoll-hypaque gradient in a 50-ml centrifuge tube. The tube was spun at 1,200 RPM (200 g) for 40 min. The PBMC at the gradient/supernatant interface were collected and washed three times with PBS. The cells were adjusted to a concentration of 7×10^6 cells/ml in PBS for the experiments.

Experimental Configurations

Individual wells were made of cut pieces of 1 ml plastic serological pipettes (3 mm inner diameter; Becton Dickinson, NJ, USA) sealed at one end with black polystyrene plates of 1.5 mm in thickness, using epoxy adhesive. Two experimental configurations were used in the experiments. The cells formed a monolayer on the bottom of the well next to the polystyrene plate (Fig. 1A) or placed on top of a solidified gelatin column 3 mm from the plate (Fig. 1B). The gelatin column was used in order to decrease the rise time of the pressure transient by allowing the pressure waves to propagate in the gelatin (8). Previous experiments have revealed that the rise time is an important parameter in the permeabilization of the plasma membrane (9).

The gelatin column was prepared as follows. A 5% gelatin solution (Knox, Nabisco, NJ, USA) prepared in PBS was injected into the wells by a 9 cm 22 G spinal needle syringe (Becton Dickinson, NJ, USA) to a height of 3 mm. After the gelatin solidified at 4°C, the PBMC were injected into the wells in both configurations, using another spindle needle syringe, and incubated at 4°C for 30 min to form a monolayer at

[1] Wellman Laboratories of Photomedicine, Department of Photopathology and Dermatology, Massachusetts General Hospital, Harvard Medical School, Boston, Massachusetts 02114.

[2] To whom correspondence should be addressed. (e-mail: tflotte@partners.org)

ABBREVIATIONS: PBS, Dulbecco's phosphate buffer solution; PBMC, peripheral blood mononuclear cell; FITC, fluorescein isothiocyanate; PI, propidium iodide.

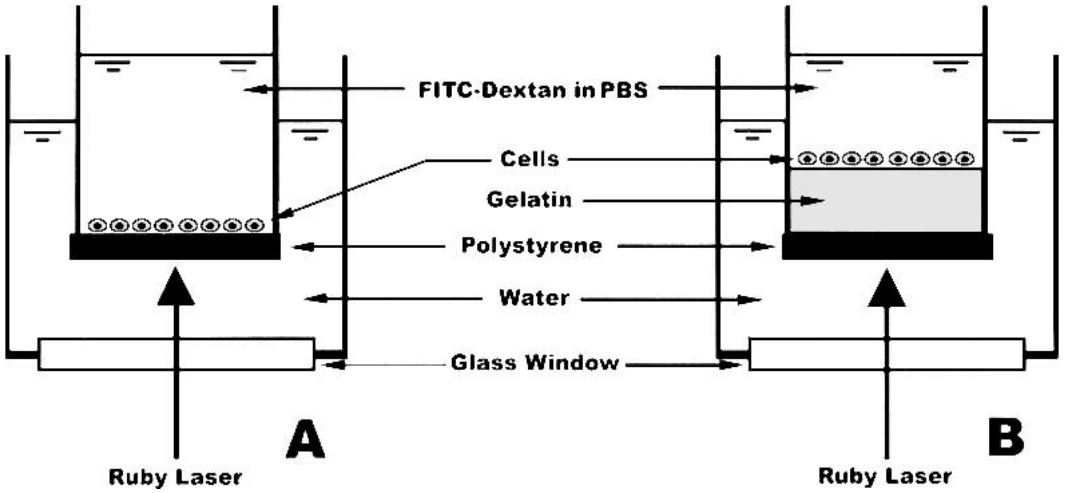

Fig. 1. Experimental configurations. Target cells (PBMC) formed a monolayer on the polystyrene plate. A pulse from the ruby laser was moderately focused on the polystyrene plate. Stress waves were produced by confined ablation of the polystyrene and launched into the medium containing the cells (A). In a second configuration, the PBMC were separated from the polystyrene plate by a 3 mm gelatin column (B).

the top of gelatin surface. There were four experiments per condition.

Then, 50 μl of 124 μM neutral fluorescein isothiocyanate (FITC)-dextran (FD-70, molecular weight 71,600 Da, Sigma, St. Louis, MO, USA) in PBS was mixed in each well with an equal volume (50 μl) of the PBMC to achieve a final concentration of 62 μM. Similarly, in the unirradiated controls, 50 μl of PBMC in PBS was incubated with 50 μl of PBS (control 1) and 50 μl of FITC-dextran (control 2), respectively. The cells in the test sample were irradiated in presence of the FITC-dextran. The cells were incubated for 30 min to form a monolayer in order to have exposure to uniform pressure waves.

Exposure of Cells to Laser-Induced Pressure Transients

The cells were exposed to pressure transients generated by laser ablation (10,11). A single pulse from a Q-switched ruby laser (RD-1200, Spectrum Medical Technologies, Natick, MA, USA) at 694.3 nm and 28 nsec duration, was steered by way of a series of mirrors and focused on the polystyrene target by a spherical lens to a spot size 2 mm in diameter. The laser pulse was totally absorbed by the target to produce a single pressure transient. The cells were not exposed to light. The fluence of ruby laser at the polystyrene plate was 53 J/cm^2. The peak pressure was estimated from previous studies using the same laser (12) and the dependence of pressure on the laser fluence reported in the literature (13). The peak pressure scales as the irradiance raised to the power of 0.7. Taking the ratio of 53 J/cm^2 and 7 J/cm^2, used in our previous work (12), and raising to the power of 0.7 gives a factor of ~4. That is, the peak pressure in our present experiments is approximately four times higher than that of our previous experiments or approximately 2 kbar. This peak pressure is the pressure generated in the target.

The non-linear propagation of a pressure wave in a medium such as gelatin causes the leading edge of the waveform to sharpen. This is the result of the dependence of the sound and particle velocity on pressure. The sound and particle velocity increases along the leading edge of the pressure wave. This causes the rise time to decrease. On the other hand, the linear attenuation, which increases as a function of frequency, attenuates predominantly the high frequency components and causes the rise time to increase. The relative strength of the linear attenuation and non-linear coefficient of the medium and the initial peak pressure, the initial rise time, and the distance traveled in the medium will determine the final value of the rise time. In this experiment, we took advantage of the non-linear propagation in gelatin to produce pressure transients with shorter rise time than can be generated by the ruby laser alone.

The propagation distance of a plane wave that will produce a shock wave can be estimated from non-linear acoustics $L = l\,\rho c^2/\varepsilon P$ (8), where l is the spatial width of the pressure transient (temporal duration multiplied by the sound velocity), ρ the density of the medium, c the sound velocity, ε the non-linear coefficient, and P the peak pressure. For the parameters of the pressure transients and assuming that the non-linear coefficient of gelatin is the same of water (approximately 1.4), the propagation distance to form a shock wave is approximately 3 mm.

After irradiation, the cells from tubes of the same sample condition were pooled together. Gelatin was thawed before aspiration by placing them in a 37°C water bath for 2 min. All samples were washed three times with PBS for 5 min each at 1200 RPM (200 g) to remove extracellular FITC-Dextran if any. After the third wash, the cells were resuspended in 1 ml of PBS. The pooled samples were placed on ice. Approximately 4 h elapsed from the time of blood draw to the time when cells were ready for examination.

Electroporation Experiments

The electroporation source was EasyjecT Optima (EquiBio, Kent, UK) with a pulse duration of a few tens of milliseconds, infinite shunt resistor and capacitor value of 1500 μF. The 72 kDa FITC-dextran (as before) was added to the PBMC to achieve a final concentration of 62 μM. The cell suspension was vortexed and incubated at room temperature for 1 to 3 min. Then 800 μL aliquots of cells were each placed into an electroporation cuvette (4 mm gap width, Eppendorf

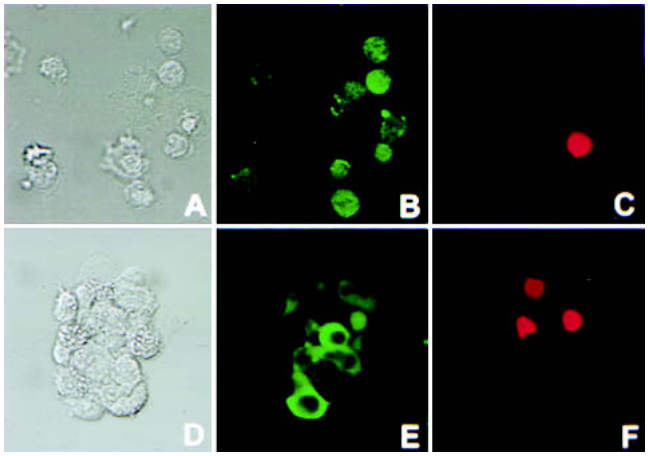

Fig. 2. Nuclear localization of the 72 kDa FITC-dextran molecules: laser-induced stress transients and electroporation for comparison. Cells exposed to laser-induced stress transients are shown in the upper panel (A, B, C), whereas the lower panel is for cells treated by electroporation (280 V) (D, E, F) (unpublished data). Images for cells under bright field (A, D) and PI-stained cells (C, F) are shown for comparison.

Scientific, Westbury, NY, USA). There were four conditions. The control sample 1 was not exposed to electroporation. The test conditions 2, 3 and 4 were each subject to an intense pulse of electric field at increasing output voltage values of 260, 280, and 300 V, respectively. Immediately (within 30 s) after electroporation, the exposed cell suspension was transferred to a centrifuge tube containing 10 mL of pre-warmed complete medium. The cells were spun at 1200 RPM for 10 min once and pellet resuspended in PBS.

In Vitro Fluorescence Confocal Microscopy

Immediately before confocal microscopy, 1 μl of propidium iodide (PI) stock solution (1 mg/ml; Molecular Probes, Eugene, OR, USA) was added to a 50 μl of cell suspension for each sample. The suspension was then plated on the glass slide and covered by a cover slip. The samples were subsequently investigated 3 min after adding PI under a commercial confocal laser scanning microscope (Leica TCS-NT, Leica Lasertechnik GmbH, Heidelberg, Germany). Scans were taken with a 40 5 oil immersion objective (PL APO, 1.25-0.75, Leica, Germany) at different zoom levels. Percentage of cell loading and that of cell death with respect to the total cell population were estimated from the images.

Data Analysis

An average fluorescence intensity per pixel was defined as the sum of fluorescence intensities in the designated area divided by the area in pixels after the background was subtracted. The background signal was derived from viable cells not loaded with the 72 kDa dextran, in the same scans as the cells of interest. The procedure was separately carried out for the cytoplasm and nucleus. The imaging processing was performed by a standard software (IPLab Spectrum 2.4.01, Signal Analytics, VA, USA) on a MacIntosh IIvx computer (Apple Computers, Cupertino, CA, USA). The average fluorescence intensity per pixel of the nucleus was compared to that of the cytoplasm using the paired *t*-test (14) for cells treated by laser.

RESULTS

Propidium iodide (PI), a vital stain, was used to label dead cells by dye exclusion. Under a fluorescence confocal microscope (Fig. 2), the nonviable cells appeared red and the viable cells loaded with FITC-dextran appeared green. Among the unirradiated controls, control 1 (see Materials and Methods) which has been incubated with PBS, the viable cells only showed intrinsic fluorescence at a level considerably less than that of FITC fluorescence. The percentage of dead cells was ~15% of the total cell population. In control 2 which has been incubated with the 72 kDa FITC-dextran, the dextran in the viable cells was localized in the cytoplasmic organelles, rather than being found throughout the cytoplasm or in the nucleus (Fig. 3). The percentage of dead cells was similar as control 1.

In the laser-irradiated test sample incubated with the 72 kDa FITC-dextran, the percentage of cells that had taken up the dextran was (10 ± 5%) when no gelatin was used and 25 ± 5% when the cells were placed on top of the 3-mm gel column. The dextran was nearly evenly distributed in both cytoplasm and nucleus of the cell. The percentage of dead cells rose to ~35% of the total cell population when the cells were exposed to a pressure transient. If only the dextran-loaded cells were considered, however, 99% of the cells remained viable.

In comparison, the fluorescence from the 72 kDa FITC-dextran was predominantly localized in the cytoplasm after electroporation, so that the loaded cells resembled "doughnuts" as evident from Fig. 2E. The FITC-stained cells were usually found in clusters. Cellular debris was widespread.

The confocal microscopic impression was supported by quantification of the ratios of nuclear to cytoplasmic concentrations of dextran. The average fluorescence intensity per pixel is proportional to the concentration of dextran molecules. Delivery with laser-induced pressure transients showed that the average fluorescence intensity per pixel in the nucleus (36 ± 16) was slightly, but statistically ($p < 0.05$ by paired *t*-test) higher than that in the cytoplasm (29 ± 13) with a ratio of nuclear to cytoplasmic concentrations of 1.2. The average background fluorescence intensity per pixel (see Materials and Methods) in the nucleus was 11 ± 7, and that in the cytoplasm was 12 ± 9.

DISCUSSION

The interaction of pressure waves with biologic tissues, cells, and macromolecules is an active area of research involv-

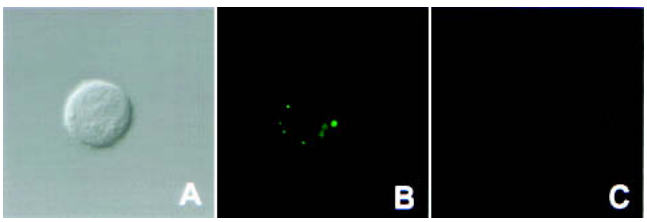

Fig. 3. Localization of the 72 kDa FITC-dextran molecules in the cytoplasmic organelles in a non-irradiated control (control 2) after incubation with the dextran: Images for cells under bright field (A), FITC-dextran-laden cells (B), and PI-stained cells (C) are shown.

ing investigators focusing on ultrasonics (15), extracorporeal shock wave lithotriptors (16–19), and photoacoustics (10,20,21). Laser-induced pressure transients have shown that these transients can produce temporary aqueous pores (9,22,23), a process we call photophonoporation. Furthermore, the cells can survive this procedure. The end result of photophonoporation is similar to that produced by electroporation (24–26).

In this work, we have demonstrated for the first time that pressure transients permealized the nuclear envelope in addition to the plasma membrane. Our results clearly showed the presence of the 72 kDa dextran in the nucleus, following the pressure transients. The dextran would otherwise be excluded of the nucleus on cytoplasmic introduction, as in electroporation (27). It is important to note that 99% of the cells that showed cytoplasmic and nuclear loading were viable. We also noted a slight, but statistically significant, nuclear localization of the dextran in the laser-treated samples. The cytoplasm is a rather complex heterogeneous composite material. The relative volume available for the diffusion of dextran molecules appeared to be less in the cytoplasm as compared with the nucleus. Since we are considering average concentrations, the unavailable "pockets" would have the effect of lowering the average concentrations.

Our work on permeabilization of the cell membrane has shown that a high pressure gradient (short rise time) is required to permeabilize the cell membrane and facilitate the delivery of macromolecules into the cytoplasm. In this work, we have investigated the potential of pressure transients for the permeabilization of the nuclear envelope. In principle, there are two ways to produce pressure transients with adjustable rise times: (1) by selecting a combination of laser wavelength and appropriate target; and (2) by taking advantage of non-linear propagation of the pressure transients in a medium. Although we have tried different combinations of lasers and targets (28), the range of the parameters of the pressure transients that are produced is limited. In these experiments, the pressure transients propagated through the gelatin in order to produce pressure transients with short rise times. We estimated the propagation length that would produce a "shock wave" from the parameters of the pressure transients generated at the target.

These experiments indicate that the permeabilization of the nuclear envelope requires a higher pressure gradient (higher peak pressure, shorter rise time or both) than the permeabilization of the plasma membrane. The fact that higher cell killing was observed at ~35% is consistent with this conclusion. In our previous work we saw no difference in cell killing between cell cultures exposed to pressure transients and control. The cell killing was practically zero. It should be pointed out, however, that even this level of cell killing (35%) is less than what has been observed during electroporation, and electroporation cannot, so far, permeabilize the nuclear envelope.

The mode of action of pressure transients in these experiments is probably quite different from that of extracorporeal shock wave (ESW) lithotripters. The ESWs have been used to permeabilize the cell membrane but there are no reports, to the best of our knowledge, of permeabilization of the nuclear envelope. The ESWs show a measurable tensile component that can produce cavitation. In fact, there are indications that cavitation plays an important role. For example, the simultaneous application of hydrostatic with ESW reduces the effectiveness of ESW for molecular delivery (29).

In gene therapy, it is hoped that human disease might be treated by transfer of genetic material into specific cells of a patient, rather than by conventional drugs (30). Methods for delivering genes into mammalian cells for either transient or stable expression are either viral or nonviral. Pressure transients provide a potentially powerful tool for gene delivery. Photophonoporation of nuclear envelopes offers unique characteristics when compared with other nonviral DNA transfection methods, such as electroporation, ligand-DNA conjugates, adenovirus-ligand-DNA conjugates, lipofection, direct injection of DNA, and calcium phosphate precipitation (30). The advantages may include *in vivo* or *in vitro* application, spatial and temporal localization, either local or distant exposure of transients, and high levels of cell survival. This may provide an opportunity for new classes of drugs because one invariant component of drug design is requirement for molecules to cross the cell membrane. Without this restriction, molecules can be designed to interact with cells in unique manners. For example, it should be possible to use this approach in combination with fiberoptic shock wave generators and catheter technology for novel drug and gene therapy in the cardiovascular system. Potentially, this technology can deliver anti-sense oligonucleotides to interrupt signals, such as the signal for smooth muscle proliferation following balloon angioplasty. This approach may also have applications in cell biology for introduction of molecules of interest into several cells while maintaining a high level of cell survival.

ACKNOWLEDGMENTS

We thank T. Kodama for invaluable discussions. This work was supported by grants from the Department of Energy, DOE-FG02-91ER61228, and from the DOD MFEL program, N00014-94-1-0927.

REFERENCES

1. R. Peters. Nuclear envelope permeability measured by fluorescence microphotolysis of single liver cell nuclei. *J. Biol. Chem.* **258**:11427–11429 (1983).
2. R. Peters, I. Lang, M. Scholz, B. Schulz, and F. Kayne. Fluorescence microphotolysis to measure nucleocytoplasmic transport *in vivo* and *in vitro*. *Biochem. Soc. Trans.* **14**:821–822 (1986).
3. I. Lang, M. Scholz, and R. Peters. Molecular mobility of nucleocytoplasmic flux in hepatoma cells. *J. Cell Biol.* **102**:1183–1190 (1986).
4. R. Peters. Nucleo-cytoplasmic flux and intracellular mobility in single hepatocytes measured by fluorescence microphotolysis. *EMBO J.* **3**:1831–1836 (1984).
5. B. Schulz and R. Peters. Nucleocytoplasmic protein traffic in single mammalian cells studied by fluorescence microphotolysis. *Biochim. Biophys. Acta* **930**:419–431 (1987).
6. M. Scholz, C. Gross-Johannböcke, and R. Peters. Measurement of nucleo-cytoplasmic transport by fluorescence microphotolysis and laser scanning microscopy. *Cell Biol. Int. Rep.* **12**:709–727 (1988).
7. S. Lee, T. Anderson, H. Zhang, T. J. Flotte, and A. G. Doukas. Alteration of cell membrane by stress waves *in vitro*. *Ultrasound Med. Biol.* **22**:1285–1293 (1996).
8. L. M. Lyamshev. Optoacoustic sources of sound. *Sov. Phys. Usp.* **24**:977–995 (1981).
9. S. E. Mulholland, S. Lee, D. J. McAuliffe, and A. G. Doukas. Cell loading with laser-generated stress waves: the role of the stress gradient. *Pharm. Res.* **16**:514–518 (1999).
10. Y. Yashima, D. J. McAuliffe, S. L. Jacques, and T. J. Flotte.

Laser-induced photoacoustic injury of skin: effect of inertial confinement. *Lasers Surg. Med.* **11**:62–68 (1991).
11. A. G. Doukas, D. J. McAuliffe, and T. J. Flotte. Biological effects of laser-induced shock waves: structural and functional cell damage *in vitro*. *Ultrasound Med. Biol.* **19**:137–146 (1993).
12. S. Lee, D. J. McAuliffe, T. J. Flotte, N. Kollias, and A. G. Doukas. Photomechanical transdermal delivery: The effect of laser confinement. *Lasers Surg. Med.* **28**:344–347 (2001).
13. C. R. Phipps Jr., T. P. Turner, R. F. Harrison, G. W. York, W. Z. Osborne, G. K. Anderson, X. F. Corlis, L. C. Haynes, H. S. Steele, K. C. Spicochi, and T. R. King. Impulse coupling targets in vacuum by KrF, HF, and CO_2 single pulse laser. *J. Appl. Phys.* **64**:1083–1096 (1988).
14. S. A. Glantz. *Primer of Biostatistics*, 3rd edition, McGraw-Hill, New York, 1992.
15. J. Liu, T. N. Lewis, and M. R. Prausnitz. Non-invasive assessment and control of ultrasound-mediated membrane permeabilization. *Pharm. Res.* **15**:918–924 (1998).
16. M. Delius and G. Adams. Shock wave permealization with ribosome inactivating proteins: a new approach to tumor therapy. *Cancer Res.* **59**:5227–5232 (1999).
17. M. Delius, F. Ueberle, and S. Gambihler. Acoustic energy determines haemoglobin release from erythrocytes by extracorporeal shock waves *in vitro*. *Ultrasound Med. Biol.* **21**:707–710 (1995).
18. S. Gambihler, M. Delius, and J. W. Ellwart. Permeabilization of the plasma-membrane of L1210 mouse leukemia cells using lithotripter shock-waves. *J. Membr. Biol.* **141**:267–275 (1994).
19. U. Lauer, E. Burgelt, Z. Squire, K. Messmer, P. H. Hofschneider, M. Gregor, and M. Delius. Shock wave permeabilization as a new gene transfer method. *Gene Ther.* **4**:710–715 (1997).
20. Y. Yashima, D. J. McAuliffe, and T. J. Flotte. Cell selectivity to laser-induced photoacoustic injury of skin. *Lasers Surg. Med.* **10**: 280–283 (1990).
21. B. J. Wong, M. R. Dickinson, and M. W. Berns. and J. Neev. Identification of photoacoustic transients during pulsed laser ablation of the human temporal bone: an experimental model. *J. Clin. Laser Med. Surg.* **14**:385–392 (1996).
22. S. Lee, D. J. McAuliffe, H. Zhang, Z. Xu, J. Taitelbaum, T. J. Flotte, and A. G. Doukas. Stress-wave-induced membrane permeation of red blood cells is facilitated by aquaporins. *Ultrasound Med. Biol.* **23**:1089–1094 (1997).
23. J. S. Soughayer, T. Krasieva, S. C. Jacobson, J. M. Ramsey, B. J. Tromberg, and N. L. Allbritton. Characterization of cellular optoporation with distance. *Anal. Chem.* **72**:1342–1347 (2000).
24. M. Bier, S. M. Hammer, D. J. Canaday, and R. C. Lee. Kinetics of sealing for transient electropores in isolated mammalian skeletal muscle cells. *Bioelectromagnetics* **20**:194–201 (1999).
25. D. C. Chang and T. S. Reese. Changes in membrane structure induced by electroporation as revealed by rapid-freezing electron microscopy. *Biophys. J.* **58**:1–12 (1990).
26. S. Y. Ho and G. S. Mittal. Electroporation of cell membranes: a review. *Crit. Rev. Biotechnol.* **16**:349–362 (1996).
27. A. Coonrod, F. Q. Li, and M. Horwitz. On the mechanism of DNA transfection: efficient gene transfer without viruses. *Gene Ther.* **4**:1313–1321 (1997).
28. D. C. Lamb, J. Tribble, A. G. Doukas, T. J. Flotte, R. H. Ossoff, and L. Reinisch. Custom designed acoustic pulses. *J. Biomed. Optics* **4**:217–223 (1999).
29. M. Delius, F. Ueberle, and W. Eisenmenger. Extracorporeal shock waves act by shock wave-gas bubble interaction. *Ultrasound Med. Biol.* **24**:1055–1059 (1998).
30. R. C. Mulligan. The basic science of gene therapy. *Science* **260**: 926–932 (1993).